


Bidirectional OFDM Based MMW/THzW Over Fiber System for Next Generation Communication

Khaleda Mallick, Paulomi Mandal, Bubai Dutta, Bibhatsu Kuiri, Saikat Santra, Rahul Mukherjee,
and Ardhendu Sekhar Patra 

Abstract—The modern world and modern technology want 5G communication to satiate their urgent need of multi-gigabits data transmission in small cells. For this aspiration, a bidirectional orthogonal frequency division multiplexing (OFDM) based millimeter wave over and terahertz wave over fiber system is proposed and demonstrated for 5G access fronthaul. A comparative study between millimeter-wave (MMW) and terahertz wave (THzW) regarding 5G communication is also analyzed. With the assistance of L and C band quantum dash laser diode, MMW and THzW are generated. For downstream (DS), 10 Gbps/12.5Gbps (for MMW/THzW) OFDM data in L band is transmitted over 50-km/25-km single mode fiber (SMF) and 100-m free space optics (FSO) distance, on the other side for upstream (US) transmission, 6.5 Gbps/10 Gbps OFDM data in C band is communicated over 50-km/25-km SMF plus 100-m FSO link. The selection of L and C band for DS and US transmission provide the advantages to reduce the Rayleigh back scattering effect in our bidirectional system not only that it also helps to mitigate the intensity-noise as compared to the conventional amplified spontaneous emission source. This research work gives an overview for the reliability of MMW and THzW system regarding 5G communication. The capability of our system becomes build up by obtaining low bit error rate (under FEC limit), proper error vector magnitude ($<10.2\%$), and clear constellation diagram.

Index Terms—Orthogonal frequency division multiplexing, millimeter wave over fiber, terahertz wave over fiber, Injection locking scheme, Quantum-dash laser diode.

I. INTRODUCTION

THE rapid growth of wireless technology from 1G to 4G is interconnected with the very fast revolution of mobile technology. There are lots of cellular networks such as Bluetooth, WLAN (wireless local area network), 3G etc remains under 4G systems, but now 4G technologies feel tired to satisfy the uncompromising demand of public [1]. Recently lots of research work is proposed to establish next generation wireless network that is 5G [2]–[4]. Our future 5G technology must be strengthen on some important sides such as bandwidth enhancement, fastest networks, small cell concepts and including some

Manuscript received May 23, 2021; revised July 28, 2021; accepted August 8, 2021. Date of publication August 16, 2021; date of current version September 6, 2021. This work was supported in part by SERB, Govt. of India under Grant CRG/2019/006580. (Corresponding author: Ardhendu Sekhar Patra.)

The authors are with the Department of Physics, Sidho-Kanho-Birsha University, Purulia 723104, India (e-mail: khaledamallick01@gmail.com; paulomimandal93@gmail.com; bubaiduttaprl@gmail.com; bibhatsu.14@gmail.com; saikatsantra6@gmail.com; rahulmukherjee89@gmail.com; ardhendu4u@yahoo.com).

Digital Object Identifier 10.1109/JPHOT.2021.3104943

new and interesting technology for communication. Our next generation 5G network is very efficient to support billions of wireless devices by the enhancement of transmission rate and capacity of the system [5], [6]. A potential alternative regarding the greater fastest indoor / hotspot connection for 5G network is found that is wireless access network at millimeter-wave (MMW) band which is famous for bandwidth enhancement [7]–[10]. Fibre optic communication support the combined form of optical fibre and wireless network as well as perform an important role very well in both backhaul and fronthaul network for future 5G access [11]. Millimetre wave over fibre (MMWOF) is very good example of wireless over fibre (WOF) system which provide numerous advantages like greater bandwidth, licence free features, high security etc which makes a potential platform to give us a comfort and easy life [12]–[16]. The outstanding entry of MMWOF into the existing network i.e., passive optical network (PON), hybrid fiber coaxial (HFC) leads to suppress the capital and operational expenditure of the system [17]. On the other hand, recently terahertz wave (THzW) band has been considered as a key technology in the world of communication system. This terahertz wave successfully overcomes the barrier of bandwidth demand of our future 5G network [18]–[21]. It is also covering a variety of applications such as medical security and scientific fields [22], [23]. During the last few years interest in this frequency range highlighted above (MMW and THzW) enhanced swiftly. Now a day's much effort is focused on the generation of MMW and THzW, and lots of research works have been proposed and demonstrated regarding the photonic generation of MMW and THzW [24], [25]. These photonic waves (MMW and THzW) are utilised properly as a powerful contestant in radio over fiber (ROF) wireless network, 5G and satellite communication [20]–[24]. There are various kind of conventional techniques reported in the communication field to generate photonic MMW and THzW, some of them are-separation of radio frequency spectrum, and optical heterodyne mixing [26], [27]. Unfortunately, the overall system cost becomes very higher for radio frequency separation scheme [26]. Whereas heterodyne scheme also offers some disadvantages such as relatively high phase noise, line width broadening and spectral purity decreasing etc. [28]. Therefore, optical injection and injection locking techniques spread their helping hand towards the heterodyne mixing scheme to eliminate the drawbacks associated with it [29]–[32]. External injection and self-injection locking both are attracted as an eminent technique due to its various advantages. The external injection-locking scheme provide the solution of

wide linewidth problem, and the amplitude and offset frequency of the perturbing optical field can be controlled by using independent laser source, but sometimes the modulation bandwidth can be hampered by it [33], [34]. Whereas the self-injection locking scheme offers high side mode suppression ratio (SMSR), large bandwidth, large capacity, cost-effectiveness, and also reduce the channel crosstalk [35], [36]. By merging the capacity of the external injection locking with the ubiquity and mobility of self-injection locking, hybrid injection locking scheme provide a powerful platform to support next generation communication system. On the other side several approaches that are based on quantum dash (Q dash) InAs /GaAs and InAs /InP laser diode (LD) for MMW and THzW applications have been proposed. Such as, MMW signal generation using Quantum dash mode locked lasers [37], 134 GHz pulse generation using a quantum-dash-based Fabry-Perot laser emitting at $1.56 \mu\text{m}$ [38] and 50 GHz/100 GHz MMW is generated with the assistance of InP based QD-LD [39]. Nevertheless, it is necessary to construct a more reliable and flexible MMWOF and THzWOF system towards our 5G communication.

This research work proposed and demonstrated an orthogonal frequency division multiplexing (OFDM) based bi-directional MMWOF and THzWOF transport system for 5G communication. A comparative study between MMWOF and THzWOF is also demonstrated here. By utilising properly, the self-injection as well as external injection locking techniques with the help of InAs /InP Quantum dash laser diode (Q dash LD), 60 GHz MMW and 1.3 THz, 1.1THz wave is generated. L and C band Quantum dash laser is used in downstream (DS) and upstream (US) communication. 10 Gbps/12.5 Gbps OFDM data (10 Gbps for MMW and 12.5 Gbps for THzW) is transmitted in downlink over 50-km/25-km single mode fiber (SMF) (50-km for MMW and 25-km for THzW) and 100-m wireless distance, and 6.5 Gbps/10 Gbps (for MMW/THzW) OFDM data is transmitted in uplink over another 50-km/25-km SMF and 100-m wireless distance. Good Bit error rate (BER) value, proper error vector magnitude (EVM), and clear constellation diagram convey the fruitful transmission of the proposed system. A conclusion to select proper system is attained towards long reach and higher capacity 5G access fronthaul networks. Best of our knowledge, this is the first time that a comparative study between OFDM based MMW/THzW for 5G network is demonstrated properly.

II. EXPERIMENTAL SETUP

Fig. 1(a) illustrates the experimental setup of the generation of photonic L and C band MMW and THzW source. L and C band Q dash LD is utilized as an optical source due to its flat and wide spectrum. 360 mA-biased L band and 300 mA-biased C band InAs/InP based Qdash LDs are used as a broad band source, the out-put power of L and C band Qdash LD is 15 mW (for L band) and 10 mW (for C band) respectively. L and C band Qdash LD ranging from 1600 nm to 1620 nm (L band) and 1554 nm to 1562 nm (C band) respectively. The light wave coming from both (L and C) of the Q dash LD is fed into one port of optical circulator (OC) via polarization controller (PC). Now these optical signals are amplified by an erbium

doped fiber amplifier (EDFA) as a booster amplifier via another port of OC. After that, the optical signal is splitted into two halves by using a 50:50 coupler (CP1). A tunable optical band pass filter (TOBPF) is connected in the feedback path of the one half of the optical signal. TOBPF controls the multiple modes power which is re-injected into the laser active medium. Finally, the selected optical mode is fed into port 3 of the OC using another 50:50 coupler (CP2) for the re-injection scheme into laser active medium. The self-injection locking scheme is successfully realized by locking the desired selected wavelength of the quantum dash emission by properly maintaining all the parameters of the instruments used here specially the central wavelength as well as the bandwidth of the band pass filter (BPF) and polarization angle of PC, etc. On the other side, tunable laser is taken for external injection locking. First of all, the light wave of this laser is fed into an optical isolator (OI) and then CP2 after that it goes into the active medium of Q dash LD through port 3 of OC. The selected desired wavelength of tunable master laser matches the fabry perot (FP) mode of Q dash LD for external injection locking with greater injection ratio. Lastly, in CP2 both the selected wavelength (self-injection and external injection wavelength) is combined to generate MMW and THzW source. Therefore, the L band MMW/THzW is modulated with 10 Gbps/12.5 Gbps OFDM data rate with the assistance of a phase modulator (PM). The OFDM data stream is generated by MATLAB programming and using an arbitrary wave form generator (AWG) with 8-bit resolution, 512-point FFT, 12 GS/s, 1/64 CP, 32 QAM modulation format. The number of subcarrier and bandwidth is 128 and 2.5 GHz. The generated OFDM data is fed into the electrical port of PM before being amplified by a linear modulator driver amplifier followed by a bias tee (bias current = 72 mA). Therefore, in PM the electrical OFDM data is modulated with our generated MMW/ THzW signal without any bias drifting problem and the peak-to-peak voltage of light wave and the half wave voltage ($V\pi$) of PM are chosen 3.5V and 12V respectively to successfully execute the modulation process. Fig. 1(b) shows the experimental setup of our bidirectional system where MMW/THzW is transmitted over 50-km/25-km SMF and 100-m free space optics (FSO) distances. After modulation with 10 Gbps/12.5 Gbps OFDM data, the L band MMW/THzW is fed into a combiner, where it is combined with C band MMW/THzW. Then, the combined wave transmitted over 50-km/25-km SMF after amplification by EDFA. The L and C band are separated by a separator in the receiving section. L band MMW/THzW is routed through one port of separator and communicated over 100-m FSO link employing doublet lens technique. At the end of FSO transmission the MMW signal is detected by 60-GHz photo diode (PD) and then filtered by a BPF.

Finally, the signal is fed into a real-time scope (DSA) and the downlink data is recovered by offline Digital Signal Processing (DSP) method. The THz wave is detected by a zero-bias detector (ZBD) followed by BPF and low noise amplifier (LNA) at the end of FSO link. The THzW is down converted by a local oscillator (LO) and a mixer and then the data is recovered with the assistance of clock data recovery (CDR). Finally, the signal is fed into bit error rate tester (BERT) to analyze the performance.

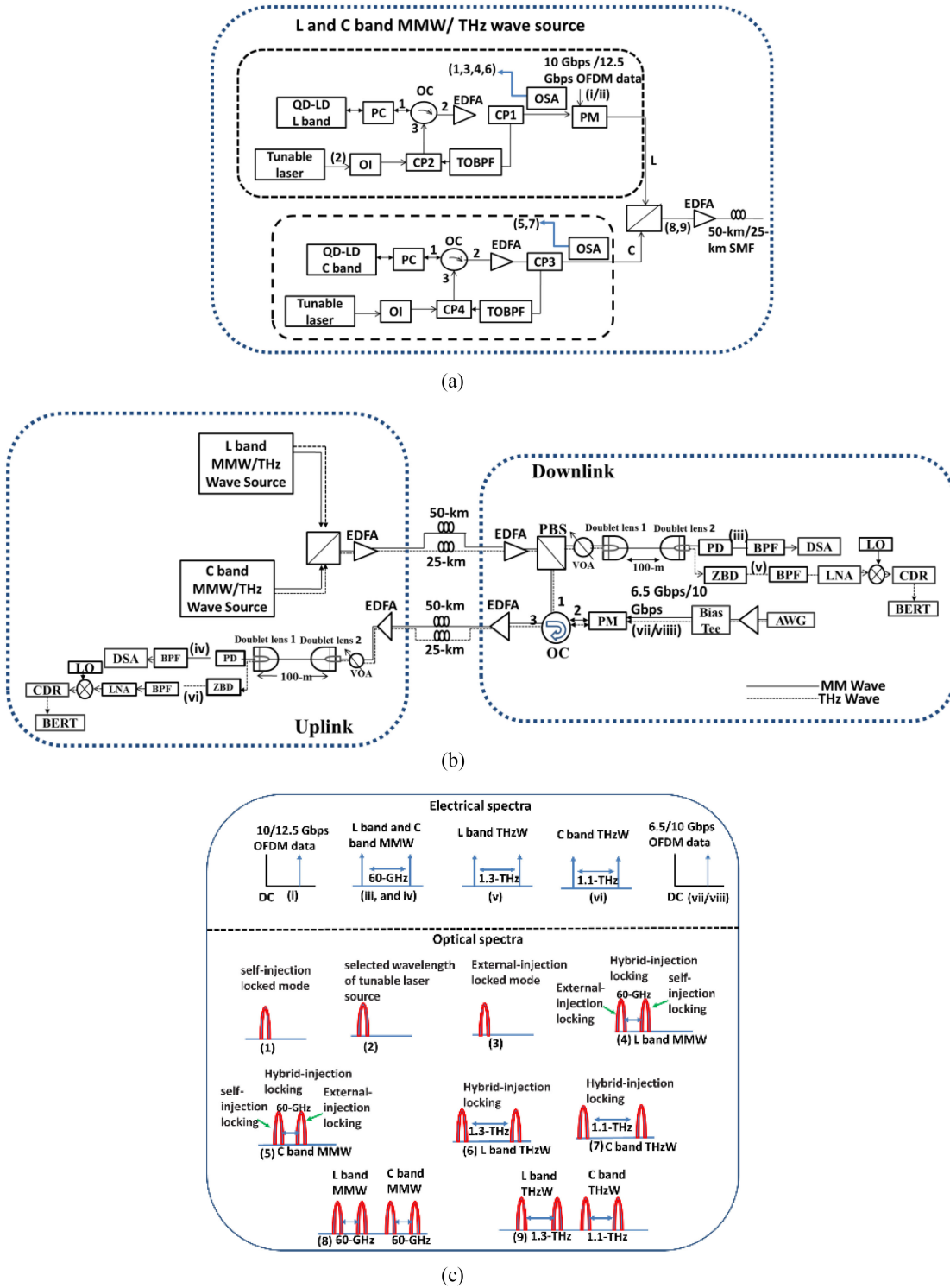


Fig. 1. (a) Schematic diagram of the generation of Land C band MMW/THzW source. (b) Experimental setup of our proposed bidirectional OFDM based MMW/THzW system. (c) Conceptual diagram of electrical and optical spectra at some points of the electrical and optical path [insert (i)–(viii) and (1)–(9) of Fig. 1(a) and Fig. 1(b)].

On the other side, the C band is routed through another port of the separator and fed into a PM via OC for uplink data modulation. In PM, C band MMW/THzW is modulated with 6.5 Gbps/10 Gbps OFDM data. After modulation, the uplink signal is fed into another 50-km/25-km SMF (MMW/THzW)

by OC. Two different SMF is used to avoid Rayleigh back scattering effect (RBS) in the bi-directional system. At first the uplink signal is amplified by EDFA and then attenuated by variable optical attenuator (VOA). Now the signal is wirelessly transmitted through the same FSO link. At the end of wireless

distance uplink MMW signal is received by a PD and fed into a BPF to filter out the unwanted noise. Therefore, finally the uplink data is launched into an OFDM analyser to analysing the transmission performance. Finally, the uplink raw data is collected by DSP method. The uplink THzW signal is detected by the ZBD after travelling through FSO link and then fed into BPF and LNA. Therefore, the THzW is down converted and fed into the BERT to evaluate its transmission performance.

Fig. 1(c) illustrates the point-to-point description of the generation of MMW and THzW signal. First, self-injection locking scheme is performed and analyzed by optical spectrum analyzer (OSA) then external injection locking scheme is distinctly executed and evaluated by OSA. After that finally both the self-injection and external injection locking scheme is carried out simultaneously to realize hybrid injection locking scheme. The inset (1) shows the self-injection locked mode (1608 nm for L band and 1555 nm for C band MMW), which is achieved by properly tuning the FP mode from the Q dash LD (QDLD) emission via a TOBPF and reinjected it into the active region of QDLD via OC. Inset (2) shows the desired wavelength selected from tunable laser source before external injection locking. After that, this selected wavelength is fed into the active region of QDLD vis CP2 followed by OC to obtain external injection locked mode (1607.52 nm for L band and 1555.48 nm for C band MMW) which shown in inset (3). Inset (4) represents the hybrid injection locking scheme, when both self-injection and external injection locking scheme is taking place simultaneously to generate L band MMW. Inset (5) shows the hybrid injection locking scheme for C band MMW. The generation of L band THzW (self-injection at 1608 nm and external injection at 1595.67 nm) and C band THzW (self-injection at 1555 nm and external injection at 1545.5 nm) with the assistance of this hybrid injection locking scheme is shown in inset (6) and (7) respectively. inset (8) and (9) show the combined form of L and C band MMW as well as THzW signal before fed into the SMF.

In this bi-directional system, at first, we generate MMW by selecting injection locked wavelength (both self and external injection locking) in a proper way and then this MMW is transmitted through the proposed bi-directional system and evaluate its transmission performance. After that, we have generated THzW by properly selecting the central wavelength of the BPF as well as tunable laser. Then this THzW is passed through the proposed architecture and evaluated its communication competence. The optical spectra show the successful generation of MMW and THzW. The performance of MMW and THzW is compared and analyzed by evaluating proper BER values, EVM and constellation diagrams.

III. RESULTS AND DISCUSSIONS

Fig. 2(a)–(g) shows the optical spectrum of the generation of L/C band MMW and THzW at different beat frequency.

Fig. 2(a) represents the single self-injection locked mode at 1608 nm. To achieve a successful self-injection lock technique, the pass band as well as the central wavelength of BPF is selected in that way to match the 1608 nm FP mode of L band Q dash LD with the assistance of PC. All the side modes associated with

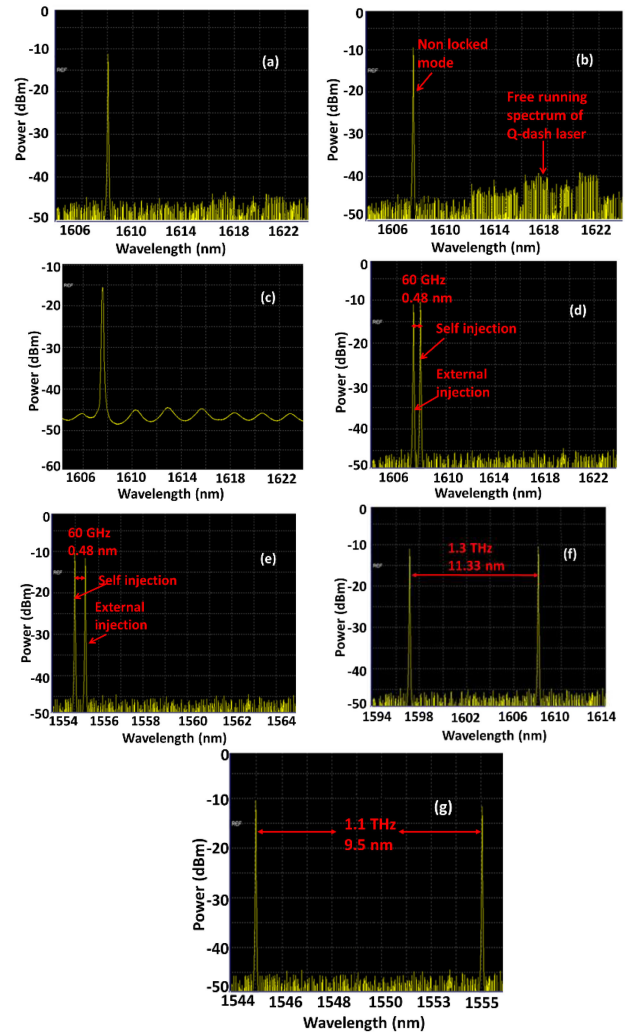


Fig. 2. (a)–(g) optical spectra of the generation of L/C band MMW and THz wave.

this wavelength are suppressed very well during self-injection locking scheme, as a result very good SMSR ~ 40 dB is achieved. Fig. 2(b) shows the optical spectrum of selected wavelength of tunable laser source (master laser) just before the external injection locking scheme. The optical spectrum of external injection locked mode at 1607.52 nm (60 GHz away from self-injection locked mode) by properly tuning master laser with SMSR ~ 29 dB, is shown in Fig. 2(c). The combined form of self-injection and external injection locked mode at 1608 nm and 1607.52 nm is displayed in Fig. 2(d). On the other word, Fig. 2(d) represents the L band 60 GHz MMW signal. Fig. 2(e) shows the optical spectrum of C band 60 GHz MMW signal. Following the same process of the generation of L band MMW, C band self-injection mode at 1555 nm and external injection mode at 1555.48 nm (60 GHz away from the self-injection locked mode) are combined to produce C band 60 GHz MMW. In case of L/C band THz wave, the external seeding wavelength was varying for external injection locked mode, keeping fixed the self-injection locked mode (both for L and C band). Fig. 2(f) and 2 (g) displays the L band 1.3 THz and C band 1.1 THz wave. For L band,

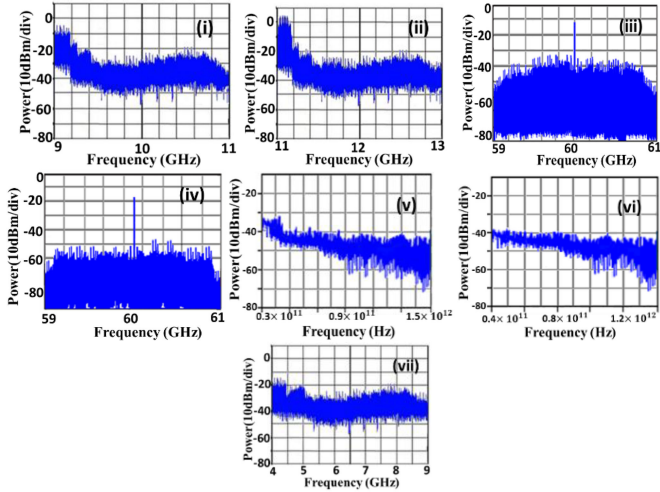


Fig. 3. (i)–(vii) Electrical spectra at some points of the electrical path [insert (i)–(vii) of Fig. 1(a) and Fig. 1(b)].

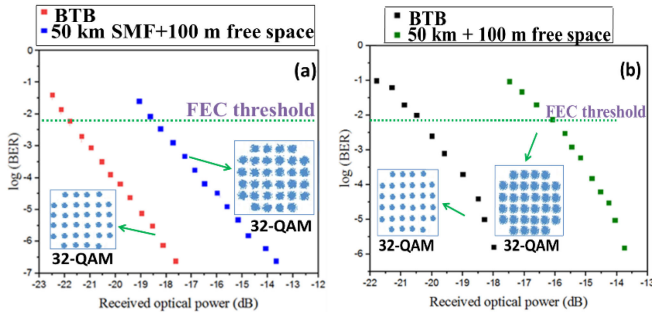


Fig. 4. Measured BER curve for (a) 10 Gbps/60 GHz MMW (L band) downlink signal and (b) 6.5 Gbps/60 GHz MMW (C band) uplink signal.

self-injection locked mode is fixed at 1608 nm and the wavelength of selected external injection mode is 1595.67 nm. For C band, 1555 nm wavelength is fixed for self-injection locking and the wavelength 1545.5 nm is selected for external injection locking. The entire optical spectra of Fig. 2 are an evidence of the successful generation of L/C band MMW and THZW. A comparative study between the L/C band MMW as well as L/C band THZW is studied by evaluating BER performance of the system. Fig. 3 (i)–(vii) represents the electrical spectra at every key node of the electrical path which reveals the fruitful transmission of the generated MMW and THZW signal.

Fig. 4(a) and 4(b) represents the measured BER curve for 10 Gbps downlink and 6.5 Gbps uplink MMW transmission with clear constellation diagram, respectively. In case of downlink signal, the receiver sensitivity is ~ -18.5 dB with a BER of 3.8×10^{-3} (under FEC limit). The recorded power penalty between back-to-back (BTB) and 50-km SMF plus 100-m FSO link is ~ 4 dB. For, uplink MMW signal, the receiver sensitivity is ~ -16.1 dB with a BER of 3.4×10^{-3} (under FEC limit). A ~ 4.5 dB power penalty is observed between BTB and 50-km SMF and 100-m FSO link, at a BER of 10^{-3} . From the BER curve, the power penalty difference between DS and US signal is very low (~ 0.5 dB). By using OFDM signal and two different bands (L and C) for DS as well as US transmission, plays

a vital role to reduce the power penalty difference between DS and US case. OFDM signal eliminates the inter symbol interference (ISI), dispersion, multipath fading effect [40], [41] and on the other side modulation into two different band for DS and US transmission simultaneously reduced the RBS effect [42], intensity-noise, and power degradation of US signal [43].

The OFDM signal is represented as [44],

$$\psi(t) = \sum_{i=-\infty}^{+\infty} \sum_{k=1}^{N_S} s_k \rho_k(t) \quad (1)$$

$$\rho_k(t) = \begin{cases} e^{j2\pi \frac{F_k}{N_s} k (t - T_s)}, & 0 \leq t \leq T_s \\ 0, & \text{otherwise} \end{cases} \quad (2)$$

Where, $\rho_k(t)$ represents the wave form of the k th subcarriers, s_k is the symbol of the k th subcarrier, F_k is the frequency of the subcarriers, T_s represent the symbol period, N_S is the number of subcarriers.

The OFDM signal is always able to overcome the inter carrier interference (ICI) effect as it is constantly follow the orthogonality condition. The condition is given by [41],

$$\frac{1}{T_s} \int_0^{T_s} \exp(j2\pi (f_k - f_n) t) dt = \begin{cases} 1, & \forall \text{ integer } k = n \\ 0, & \text{otherwise} \end{cases} \quad (3)$$

A major part of OFDM signal is the length of cyclic prefix (CP), called guard interval. After introducing CP at every symbol, the total symbol duration is enhanced, such as [44],

$$T_{total} = T_{CP} + T_s \quad (4)$$

Where, T_{CP} is the length of the CP.

The length of the CP is taken longer than the maximum delay of the multipath channel in wireless link, the signal is obeying a certain condition such as [4],

$$t_{delay} < \delta_G \quad (5)$$

Where, δ_G is the guard interval between the symbols.

Therefore, the OFDM signal is represented as,

$$\psi(t) = \sum_{i=-\infty}^{+\infty} \sum_{k=1}^{N_S} s_k \psi_{ik}(t) - T_{CP} \leq t \leq T_s \quad (6)$$

CP is removed from every symbol in the OFDM receiver and at the same time all the ISI from the previous symbol which is carried by the CP is also removed. As a result, dispersion as well as ISI free signal is achieved.

On the other hand, the OFDM signal can easily overcome the fading effect due to its frequency selective fading response. By analysing the frequency selective response of OFDM spectrum, it is noticed that only one or two subcarriers are affected by fading, due to this reason a small sub-set of bit stream is lost not the whole data rate [45].

Fig. 5(a) and (b) represent the BER vs receive optical power graph for 12.5 Gbps/1.3 THZW DS signal and 10 Gbps/1.1 THZW US signal transmission over 25-km SMF plus 100-m (for DS) and 100-m (for US) wireless distance, respectively. For DS transmission, ~ -16.6 dB receiver sensitivity with a BER of 3.2×10^{-3} is obtained. The power

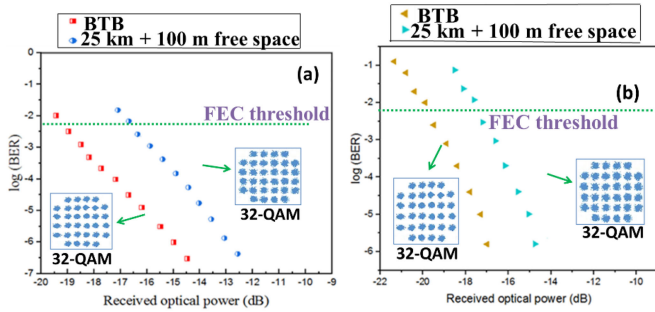


Fig. 5. BER vs receive optical power graph for (a) L band 12.5 Gbps/1.3 THzW DS signal and (b) C band 10 Gbps/1.1 THzW US signal.

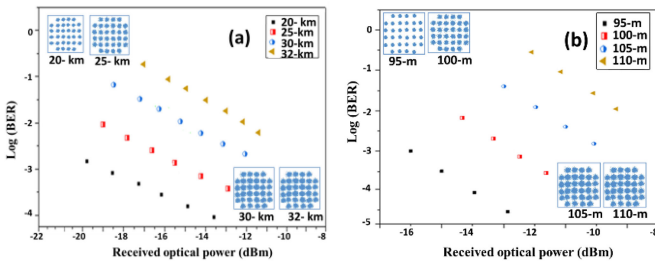


Fig. 6. Measured BER curve for (a) 1.3 THzW over 20-km/25-km/30-km/32-km SMF and (b) over 95-m/100-m/105-m/110-m wireless link.

penalty of ~ 2 dB is achieved for DS signal. Other side for, ~ -16.9 dB receiver sensitivity with a BER of 2.8×10^{-3} is recorded for US transmission. The power penalty between BTB and 25-km SMF plus 100-m FSO link for uplink transmission is ~ 2.3 dB. The clear constellation diagrams are also depicted in Fig. 5. The BER vs receive optical power graph at different transmission distances (SMF and wireless distances) is recorded to analyze the capability of generated THzW for long reach communication. Fig. 6(a) and (b) represent the measured BER curve at various distances. From Fig. 6(a) and (b), it is clear that when transmission distance is larger than 25-km SMF and larger than 100-m wireless distance the BER value exceeds the FEC limit (greater than 10^{-3}) with messy and noisy constellation diagrams. The reason behind the problem highlighted above is the greater amount of attenuation, which arises because of the very strong scattering and absorption by atmosphere due to rain, dust, clouds, etc. [46]–[49].

On the other hand, to examine the capacity of generated MMW signal, the transmission data rate slightly increases for both DS and US communication. Fig. 7(a) and (b) represent the measured BER curve for 12.5 Gbps for DS and 10 Gbps for US transmission. Now, for this experiment we take the same data rate as that of the THzW for better comparison. From this experiment, it is noted that when we increase the data rate the BER value till maintain the FEC limit, but the power penalty become so high (~ 5.4 dB for DS and ~ 6.5 dB for US) as compared to the estimated value. The achieved values of this experiment do not convey a clear signature of fruitful transmission. From the graphs Fig. 4–Fig. 7, the MMW is suitable for long reach 5G communications with moderated data rate (not very low, not so

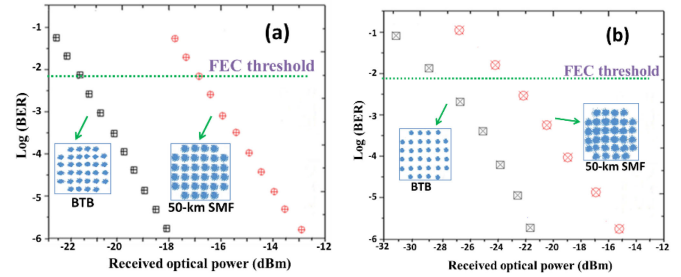


Fig. 7. Measured BER curve for (a) 12.5 Gbps/60 GHz MMW downlink signal and (b) 10 Gbps/60 GHz MMW uplink signal.

high), on the other side THzW is a potential candidate regarding higher capacity but with small 5G communication distance.

IV. CONCLUSION

In this study, a novel bidirectional OFDM based MMWOF and THzWOF system is established for the evaluation of MMW and THzW towards 5G access fronthaul network. L and C band Q dash LD act as a broadband source for downlink and uplink transmission respectively to generate MMW and THzW beat frequency. L band downlink signal is transmitted with 10 Gbps data rate (via MMW) as well as 12.5 Gbps data rate (via THzW) and C band uplink signal is communicated with 6.5 Gbps data rate (via MMW) as well as 10 Gbps data rate (via THzW). A detailed comparative study between MMW and THzW regarding data rate transmission capacity and the capability of long reach communication for 5G network is also demonstrated. The efficiency of the system is evaluated by low BER (10^{-3} under FEC limit), proper EVM ($< 10.2\%$) and clear constellation diagram. Based on the results, it can be concluded that MMW and THzW both are very strong and powerful candidate for 5G communication for different requirement. In case of long reach 5G communications, MMW is suitable contender and for higher transmission capacity but limited propagation length, THzW will always play a vital role for 5G communications. The presented architecture can promote the deployment of next generation communication system.

ACKNOWLEDGMENT

The authors would like to acknowledge the infrastructural facility provided by Sidho-Kanho-Birsha University, Purulia, India.

REFERENCES

- [1] S. Y. Hui and K. H. Yeung, "Challenges in the migration to 4G mobile systems," *IEEE Commun. Mag.*, vol. 41, no. 12, pp. 54–59, Dec. 2003.
- [2] J. G. Andrews *et al.*, "What will 5G be?," *IEEE J. Sel. Areas Commun.*, vol. 32, no. 6, pp. 1065–1082, Jun. 2014.
- [3] A. Osseiran *et al.*, "Scenarios for 5G mobile and wireless communications: The vision of the METIS project," *IEEE Commun. Mag.*, vol. 52, no. 5, pp. 26–35, May 2014.
- [4] L. Cheng, M. Zhu, M. M. U. Gul, X. Ma, and G.-K. Chang, "Adaptive photonics-aided coordinated multipoint transmissions for next-generation mobile fronthaul," *J. Lightw. Technol.*, vol. 32, no. 10, pp. 1907–1914, May 2014.

- [5] F. Boccardi, R. W. Heath, A. Lozano, T. L. Marzetta, and P. Popovski, "Five disruptive technology directions for 5G," *IEEE Commun. Mag.*, vol. 52, no. 2, pp. 74–80, Feb. 2014.
- [6] C. Y. Li *et al.*, "Generation and transmission of BB/MW/MMW signals by cascading PM and MZM," *J. Lightw. Technol.*, vol. 30, no. 3, pp. 298–303, Feb. 2012.
- [7] Y. T. Hsueh, Z. Jia, H. C. Chien, J. Yu, and G. K. Chang, "A novel bidirectional 60-GHz radio-over-fiber scheme with multiband signal generation using a single intensity modulator," *IEEE Photon. Technol. Lett.*, vol. 21, no. 18, pp. 1338–1340, Sept. 2009.
- [8] F. Lecoche *et al.*, "Transmission quality measurement of two types of 60 GHz millimeter-wave generation and distribution systems," *J. Lightw. Technol.*, vol. 27, no. 23, pp. 5469–5474, Dec. 2009.
- [9] G. Chang and C. Liu, "1–100 GHz microwave photonics link technologies for next-generation WiFi and 5G wireless communications in microwave photonics (MWP)," in *Proc. IEEE Int. Topical Meeting Microw. Photon.*, 2013, pp. 5–8.
- [10] Y. Niu, Y. Li, D. Jin, L. Su, and A. V. Vasilakos, "A survey of millimeter wave (mm wave) communications for 5G: Opportunities and challenges," in *Proc. Wireless Netw.*, 2015, pp. 2657–2676.
- [11] K. Mallick, R. Mukherjee, B. Das, G. C. Mandal, and A. S. Patra, "Bidirectional hybrid OFDM based wireless-over-fiber transport system using reflective semiconductor amplifier and polarization multiplexing technique," in *Proc. Int. J. Electron. Commun.*, 2018, pp. 260–266.
- [12] C. Y. Lin *et al.*, "Millimeter-wave carrier embedded dual-color laser diode for 5G MMW of link," *J. Lightw. Technol.*, vol. 35, no. 12, pp. 2409–2420, Jun. 2017.
- [13] S. E. Alavi *et al.*, "Towards 5G: A photonic based millimeter wave signal generation for applying in 5G access fronthaul," in *Proc. Sci. Rep.*, 2016, Art. no. 19891.
- [14] K. Mallick, P. Mandal, G. C. Mandal, R. Mukherjee, B. Das, and A. S. Patra, "Hybrid MMW-over fiber/OFDM-FSO transmission system based on doublet lens scheme and POLMUX technique," *Opt. Fiber Technol.*, vol. 52, 2019, Art. no. 101942, doi: [10.1016/j.yofte.2019.101942](https://doi.org/10.1016/j.yofte.2019.101942).
- [15] H. Shams, P. Perry, P. M. Anandarajah, and L. P. Barry, "Modulated millimeter-wave generation by external injection of a gain switched laser," *IEEE Photon. Technol. Lett.*, vol. 23, no. 7, pp. 447–449, Apr. 2011.
- [16] K. Mallick, P. Mandal, R. Mukherjee, G. C. Mandal, B. Das, and A. S. Patra, "Generation of 40 GHz/80 GHz OFDM based MMW source and the OFDMFSO transport system based on special fine tracking technology," *Opt. Fiber Technol.*, vol. 54, no. 9, 2020, Art. no. 102130.
- [17] Y. Xiang, N. Jiang, C. Chen, C. Zhang, and K. Qiu, "Wired/wireless access integrated RoF-PON with scalable generation of multi-frequency MMWs enabled by tunable optical frequency comb," *Opt. Exp.*, vol. 21, no. 17, pp. 19762–19767, 2013.
- [18] H. Song *et al.*, "Terahertz wireless communication link at 300 GHz," in *Proc. IEEE Int. Topical Meeting Microw. Photon.*, 2010, pp. 42–45.
- [19] T. Kleine-Ostmann, K. Pierz, G. Hein, P. Dawson, and M. Koch, "Audio signal transmission over a THz communication channel using semiconductor modulator," *Electron. Lett.*, vol. 40, no. 2, pp. 124–126, 2004.
- [20] Y. C. Shen, P. C. Upadhyaya, E. H. Linfield, H. E. Beere, and A. G. Davies, "Ultrabroadband THz radiation from low-temperature grown GaAs photoconductive emitters," *Appl. Phys. Lett.*, vol. 83, pp. 3117–3119, 2003.
- [21] D. Grischkowsky, S. Keiding, M. van Exter, and C. Fattinger, "Far-infrared time-domain spectroscopy with terahertz beams of dielectrics and semiconductors," *J. Opt. Soc. B*, vol. 7, no. 10, pp. 2006–2015, 1990.
- [22] P. H. Siegel, "Terahertz technology in biology and medicine," *IEEE Trans. Microw. Theory Techn.*, vol. 52, no. 10, pp. 2438–2447, Oct. 2004.
- [23] D. Grischkowsky and R. A. Cheville, "Limits and applications of THz time-domain spectroscopy," in *Proc. SPIE—Int. Soc. Opt. Eng.*, 1995, pp. 26–37.
- [24] T. Nagatsuma *et al.*, "Millimeter- and THz-wave photonics towards 100-Gbit/s wireless transmission," in *Proc. 23rd Annu. Meeting IEEE Photon. Soc.*, 2010, pp. 385–386.
- [25] F. D. J. Brunner, S.-H. Lee, O.-P. Kwon, and T. Feurer, "THz generation by optical rectification of near-infrared laser pulses in the organic nonlinear optical crystal HMQ TMS," *Opt. Mater. Exp.*, vol. 4, no. 8, pp. 1586–1592, 2014.
- [26] G. Carpintero, R. C. Guzman, C. G. on, G. Kervella, M. Chitoui, and F. V. Dijk, "Photonic integrated circuits for radio-frequency signal generation," *J. Lightw. Technol.*, vol. 34, no. 2, pp. 508–515, Jan. 2016.
- [27] H.-Y. Chen, Y.-C. Chi, and G.-R. Lin, "Remote heterodyne millimeter-wave over fiber based OFDM-PON with master-to-slave injected dual-mode colorless FPLD pair," *Opt. Exp.*, vol. 23, no. 17, pp. 22691–22705, 2015.
- [28] F. Paresys, T. Shao, G. Maury, Y. L. Guennec, and B. Cabon, "Bidirectional millimeter-wave radio-over-fiber system based on photodiode mixing and optical heterodyning," *IEEE/OSA J. Opt. Commun. Netw.*, vol. 5, no. 1, pp. 74–80, Jan. 2013.
- [29] M. K. Hong, Y. Y. Won, and S. K. Han, "Gigabit optical access link for simultaneous wired and wireless signal transmission based on dual parallel injection-locked Fabry-Pérot laser diodes," *J. Lightw. Technol.*, vol. 26, no. 15, pp. 2725–2731, Aug. 2008.
- [30] Y. F. Wu, C. H. Yeh, C. W. Chow, Y. F. Shih, and S. Chi, "Employing external injection-locked Fabry-Perot laser scheme for MMW generation," *Laser Phys.*, vol. 21, no. 4, pp. 718–721, 2011.
- [31] G. C. Mandal, R. Mukherjee, B. Das, and A. S. Patra, "Bidirectional and simultaneous transmission of baseband and wireless signals over RSOA based WDM radio-over-fiber passive optical network using incoherent light injection technique," *AEU—Int. J. Electron. Commun.*, vol. 80, pp. 193–198, 2017, doi: [10.1016/j.aeue.2017.07.030](https://doi.org/10.1016/j.aeue.2017.07.030).
- [32] C.-Y. Lin, Y.-C. Chi, C.-T. Tsai, H.-Y. Chen, and G.-R. Lin, "Two-color laser diode for 54-Gb/s fiber-wired and 16-Gb/s MMW wireless OFDM transmissions," *Photon. Res.*, vol. 5, no. 4, pp. 271–279, 2017.
- [33] E. Sooudi *et al.*, "Injection-locking properties of InAs/InP based mode-locked quantum-dash lasers at 21GHz," *IEEE Photon. Technol. Lett.*, vol. 23, no. 20, pp. 1544–1546, Oct. 2011.
- [34] T. B. Simpson, J. M. Liu, K. F. Huang, and K. Tai, "Nonlinear dynamics induced by external optical injection in semiconductor lasers," *Quantum Semiclassical Opt.: J. Eur. Opt. Soc. Part B*, vol. 9, no. 5, 1997, Art. no. 765.
- [35] M. A. Shemis *et al.*, "L-band quantum-dash self-injection locked multi-wavelength laser source for future WDM access networks," *IEEE Photon. J.*, vol. 9, no. 5, Oct. 2017, Art. no. 7905807.
- [36] R. Mukherjee *et al.*, "PAM-4 based long-range free-space-optics communication system with self-injection locked QD-LD and RS codec," *Opt. Commun.*, vol. 476, p. 126304, 2020, doi: [10.1016/j.optcom.2020.126304](https://doi.org/10.1016/j.optcom.2020.126304).
- [37] F. V. Dijk *et al.*, "Quantum dash mode locked lasers for millimeter wave signal generation and transmission," in *Proc. 23rd Annu. Meeting IEEE Photon. Soc.*, 2010, pp. 187–188.
- [38] C. Gosset *et al.*, "Subpicosecond pulse generation at 134 GHz using a quantum-dash-based Fabry-Perot laser emitting at 1.56 μm ," *Appl. Phys. Lett.*, vol. 88, no. 24, pp. 241105–241105, 2006.
- [39] G. C. Mandal, R. Mukherjee, B. Das, and A. S. Patra, "A full-duplex WDM hybrid fiber-wired/fiber-wireless/fiber-VLC/fiber-IVLC transmission system based on a self-injection locked quantum dash laser and a RSOA," *Opt. Commun.*, vol. 427, pp. 202–208, 2018.
- [40] T. Hwang, C. Yang, G. Wu, S. Li, and G. Y. Li, "OFDM and its wireless applications: A survey," *IEEE Trans. Veh. Technol.*, vol. 58, no. 4, pp. 1673–1694, May 2009.
- [41] Y. S. Cho, J. Kim, W. Y. Yang, and C. G. Kang, "Mimo-OFDM wireless communications with matlab," in *IEEE Press, Asia: John Wiley and Sons Pte*, 2010.
- [42] T. Dong, Y. Bao, Y. Ji, A. P. T. Lau, Z. Li, and C. Lu, "Bidirectional hybrid OFDM-WDM-PON system for 40-Gb/s downlink and 10-Gb/s uplink transmission using RSOA remodulation," *IEEE Photon. Technol. Lett.*, vol. 24, no. 22, pp. 2024–2026, Nov. 2012.
- [43] Q. T. Nguyen *et al.*, "24 channels colorless WDM-PON with L-band 10 Gb/s downstream and C-band 2.5 Gb/s upstream using multiple wavelengths seeding sources based on mode-locked lasers," in *Proc. Conf. Opt. Fiber Commun. (OFC/NFOEC), Collocated Nat. Fiber Optic Engineers Conf.*, 2010, pp. 1–3.
- [44] W. Shieh, H. Bao, and Y. Tang, "Coherent optical OFDM: Theory and design," *Opt. Exp.*, vol. 16, no. 2, pp. 841–859, 2008.
- [45] R. W. Chang, "Orthogonal frequency division multiplexing," U.S. Patent, 1970, Art. no. 488445.
- [46] R. Piesiewicz *et al.*, "Short-range ultra-broadband terahertz communications: Concepts and perspectives," *IEEE Antennas Propag. Mag.*, vol. 49, no. 6, pp. 24–39, Dec. 2007.
- [47] V. Petrov, A. Pyattaev, D. Moltchanov, and Y. Koucheryavy, "Terahertz band communications: Applications, research challenges, and standardization activities," in *Proc. 8th Intern. Congr. Ultra-Modern Telecommun. Control Sys. Workshops*, 2016, pp. 18–20.
- [48] M. J. Fitch and R. Oslander, "Terahertz waves for communications and sensing," *Johns Hopkins Apl Tech. Dig.*, vol. 25, no. 4, pp. 348–355, 2004.
- [49] T. Kurner and S. Priebe, "Towards THz communications - status in research, standardization and regulation," *J. Infrared Millim. THz Waves*, vol. 35, no. 1, pp. 53–62, 2014.